Synthesis and Structural Analysis of Molybdenum Disulfide Nanoparticles by Sol-Gel Technique

Sundus S. Abrahaim and Ziad T. Khodair
Department of Physics, College of Science, University of Diyala, 32001 Baqubah, Diyala, Iraq
sundusshawkat@gmail.com, ziadtariq70@yahoo.com

Keywords: Molybdenum Disulfide, Sol-Gel, XRD, FESEM, FTIR.

Abstract: Sol-gel was used to make molybdenum disulfide nanoparticles (MoS2) for this work. X-ray diffraction (XRD), Field emission scanning electron microscopy (FESEM), and Fourier transform infrared spectroscopy (FTIR) methods were used to examine the results. The XRD test showed that the nanoparticles were hexagonal, and the Scherrer method was used to find out that the average crystallite size (Dav) of the nanoparticles that were produced was around 40 nm. According to FESEM images, the crystalline forms are heterogeneous in size and shape, and the MoS2 nanosheets stack together to form a huge block with varying internal thicknesses. The average size distribution of MoS2 is about 42 nm. These results are consistent with the XRD. FTIR measurements performed for MoS2 nanoparticles showed that the strong and weak absorption bands of the (S - S) bond are located between (543-809) cm^{-1}, while the bands located (1100-1630) cm^{-1} are due to the (Mo-S) bond, while the bands located at (2740-2357) cm^{-1} are due to the (O-H) bond.

1 INTRODUCTION

Scientists are very interested in transition metal dichalcogenides (TMDs) in two dimensions right now because they have some very interesting properties. The chemical formula for two-dimensional transition metal dichalcogenides is MX_2. Ti, chromium, manganese, zirconium, nickel, molybdenum, tectonic, hydrogen, and iron are all transition metals from Group IVB to Group VIIB, which includes M. As a chalcogen atom, X is composed of selenium, sulfur, and copper [1]. Figure 1 [2] illustrates that TMD materials can be constructed in both layered and non-layered fashions. A high surface-to-volume ratio, significant catalytic activity, a high degree of hydrophilicity, a large number of edge facets, a high chemical inertness, and a changeable band gap are some of these materials' physical and chemical characteristics. Developments in atomically thin two-dimensional transition metal chalcogenides have produced a number of exciting innovations in photonics, energy storage, nanoelectronics, sensing, and optoelectronics [3]. Molybdenum disulfide is used in solid lubricants, photovoltaics, and rechargeable batteries, among other things, because it has good optical, electrical, and mechanical properties. The crystal structure of molybdenum disulfide is hexagonal, with two sulfur layers in the middle of metal layers that are held together by weak van der Waals forces [4]. MoS_2 is a layered transition metal chalcogenide that has been studied a lot. A straight band gap of 1.8 eV is found in MoS2 when it is in a single layer [5]. It's good news that MoS_2 can mostly make up for gapless graphene's flaws, because this means that two-dimensional materials can be used in photonic and next-generation switching devices [6]. The sol-reaction method was used to make MoS2 nanoparticles for this study, and XRD and FESEM were used to look at their structural features.

2 EXPERIMENTAL DETAILS

MoS_2 nanoparticles were prepared by sol-gel method by following the following steps:

1) Sodium molybdate dihydrate $Na_2MoO_4.2H_2O$ with a 241.95 g/mol molecular weight and a density of (g/cm^3) was dissolved in deionized distilled water at a concentration of 0.1 M. Thiourea $SC(NH_2)_2$ with a purity of 99%, a molecular weight of 12.76 g/mol, and a concentration of 0.1 M, prepared by (Poole-England-General Purpose Reagent Limited), was also used. Citric acid

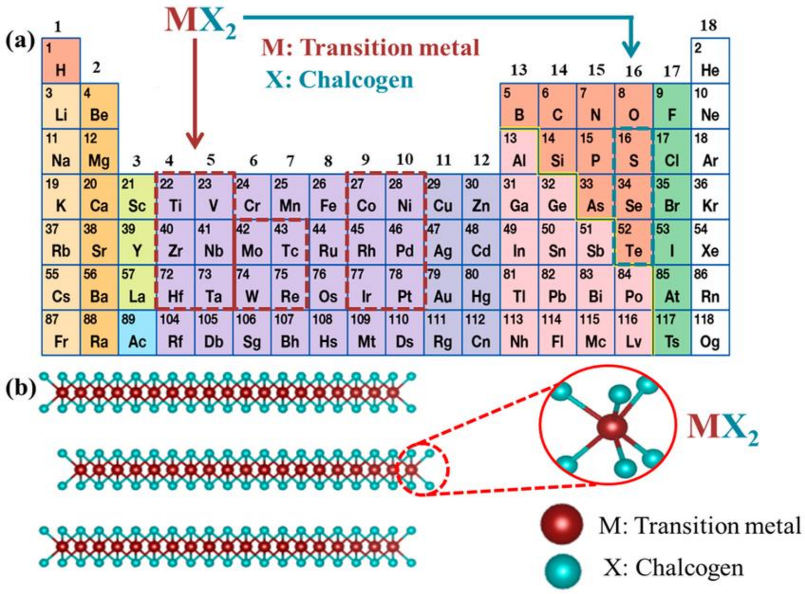

Figure 1: The components of TMDs are composed of three chalcogen atoms and sixteen transition metals [9].

with a molecular formula of C6H8O7, a concentration of 0.5 M, and a molecular weight of 192.123 g/mol was also added.

2) After completing the dissolution process, the acidity (pH) of the solution was measured and it was (pH=1.4). To make the solution neutral, ammonia solution (NH_4OH) was added at a concentration of (25%), prepared by SIGMA, in drops to the prepared solution at intermittent intervals, while the solution remained on the magnetic mixer until the solution became neutral (PH=7 ± 0.05), and the solution turned white.
3) Before the solution turned into gel, the magnetic mixer's temperature was raised until it reached 80°C. The temperature stayed the same, and the solution was left on the magnetic mixer for 40 to 50 minutes so that the liquid would slowly evaporate, as shown in Figure 2.
4) In order to eliminate all water molecules and other liquids, the resultant particles were annealed in an electric furnace set at 500°C for two hours. The particles were then left inside the furnace for two hours, and the particles were left inside the furnace for 24 hours until its temperature reached room temperature as shown in Figure 1, after that (MOS2) particles were obtained.

Figure 2. Steps for preparing MoS_2 nanoparticles by sol-gel method

3 RESULTS AND DISCUSSIONS

3.1. Results of XRD

The XRD of the produced MoS_2 nanoparticles is displayed in Figure 3. The diffraction peaks 2ϴ~14.36°, 28.96°, 32.61°, 33.42°, 39.45°, 44.05°, 49.68°, 58.18°, 60.62°, 75.83° and 88.44° have appeared. It is referred to as Miller index favored directions (002), (004), (100), (101), (103), (006), (105), (110), (114), (116), and (118), respectively. The card number (01-075-1539) of MoS_2 from the Inorganic Crystal Structure Database (ICSD) is exactly what these values correspond [7]. Additionally, results indicated the hexagonal structure of the nanoparticles.

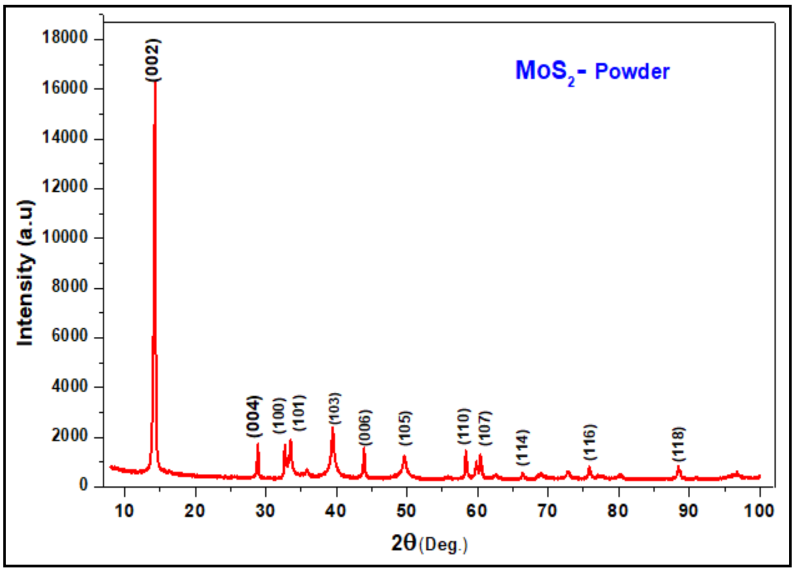

Figure 3: XRD of MoS_2 nanoparticles.

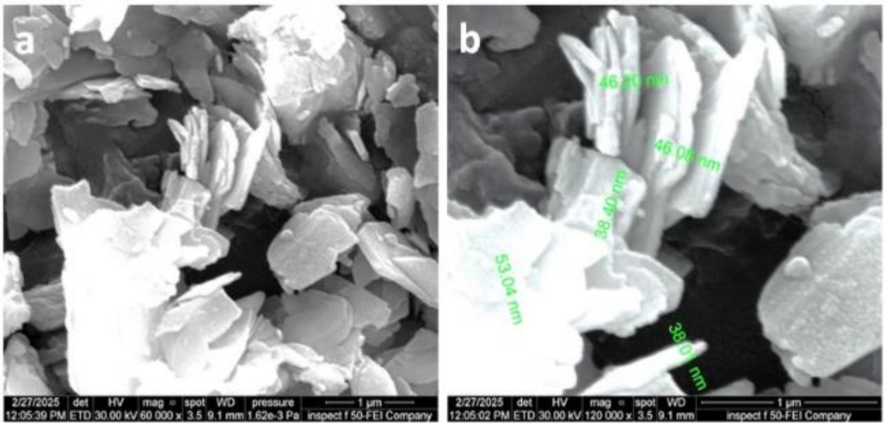

Figure 4: An FESEM image of MoS_2 nanoparticles a) and b).

Table 1: The MoS_2 nanoparticles' structural characteristics.

θ° (deg.)	d-spacing (Å)	FWHM (rad)	average crystallite size (D_{av}), (nm)	Micro Strain $*10^{-3}$	SSA ($m^2.g^{-1}$)
14.36	6.22457	0.2798	**29**	1.09295	41
28.96	3.09608	0.2058	**40**	0.34275	30
32.61	2.73764	0.2673	**31**	0.39945	38
33.42	2.67751	0.3577	**29**	0.8713	41
39.45	2.28262	0.5564	**41**	1.14817	29
44.05	2.06161	0.1965	**32**	0.2684	37
58.18	58.3337	0.1811	**50**	0.14795	59
60.62	1.53129	0.1895	**48**	0.14083	25
75.83	1.25372	0.2273	**44**	0.17428	27
88.44	1.10444	0.2442	**45**	0.13915	26

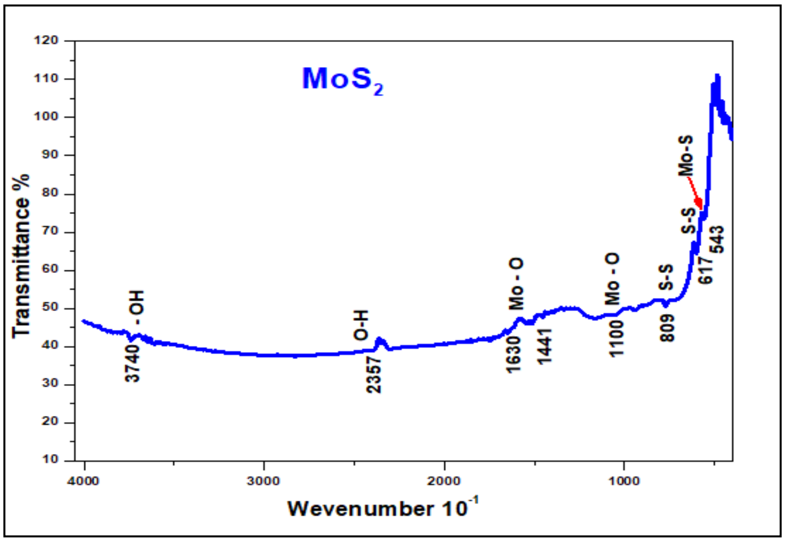

Figure 5: FTIR measurements for MoS_2 nanoparticles.

Using Bragg's law and the relation (1) [8], the distance between interplanar spacing (d_{hkl}) with the same Miller's coefficients (hkl) was computed [8] . when it was discovered that the value of (d_{hkl}) is close to and consistent with the MoS_2 standard card (ICSD card no. 75-1539) [7]

$$n\lambda = d_{hkl} \sin \Theta_B . \quad (1)$$

Where: d_{hkl} - the distance between interplanar spacing, Θ_B: Bragg angle, λ - wavelength, n - order of reflection.

For the produced MoS_2 nanoparticles, the crystal lattice constants ($a_o = b_o$, and c_o) were computed using the hexagonal structure relation, (2) [9]. Table 1 displays these values

$$\frac{1}{d^2{}_h} = \frac{4}{3}\left(\frac{h^2+hk+k^2}{a_o^2}\right) + \frac{l^2}{c_o^2} . \quad (2)$$

From planes 110 and 114, we found the lattice constants a_o and c_o. The numbers h, k, and l stand for Miller coefficients. It was found that the values of the lattice constants are the same as those on the MoS_2 international card number 75-1539. The information is shown in Table 1. We used the Scherrer method and (3) [10]–[12] to figure out the average crystallite size (Dav) of the nanoparticles that were made:

$$D_{av} = \kappa\lambda / (\beta \cos \theta^B). \quad (3)$$

The quantity of deficiencies in the crystal is measured by the dislocation density (δ). Good crystallization of MoS_2 nanoparticles made using the sol-gel approach was confirmed by the minimal dislocation density value found in this work (4) was used to compute the dislocation density [13] as shown in Table 1:

$$\delta = 1 / D_{av}{}^2. \quad (4)$$

According to one meaning, specific surface area (SSA) is the area measured in mass units (m^2/g). It determines the quality of materials and is a very significant attribute for nanomaterials. It also provides information regarding surface-level interactions [14]. The SSA values determined using the following (5) [15] are displayed in Table 1:

$$SSA = S_V / \rho . \quad (5)$$

When K_{SV} is set to 6, which is the number for a sphere, the surface density (SV) is displayed.and D_{av}, while ρ is the material density (ρ = 5.06 g/cm^3 for MoS_2 nanoparticles)., i.e., SV $= \frac{K_{sv}}{D_{av}}$. Rearranging (5) yields the following (6):

$$SSA = 6 \times 10^3 / (D_{av}\, \rho). \quad (6)$$

3.2 Analysis of FESEM

FESEM analysis was performed on the sol-gel-prepared MoS_2 nanoparticles. Figure 4a and 4b illustrates that the crystalline formations exhibit diverse, heterogeneous sizes and morphologies, and that the MoS_2 nano sheets stack together to form a large block with different internal thicknesses. These results are consistent with studies [16], [17], [18]. Figure 4b shows the average size distribution of MoS_2 approximately 42 nm. The X-ray diffraction results are in agreement with these results.

3.3 FTIR Measurements

FTIR analysis was performed on MoS_2 nanoparticles made using the sol-gel process in the 400–4000 cm^{-1} range. by computing the wavenumber dependency of the transmittance spectrum. The transmittance spectrum was measured as a function of wavenumber. Figure 5 shows relatively strong absorption bands at (543, 617, 806, 1100, 1441, 1630, 2357, and 3740) cm^{-1}. These results are consistent with studies [19], [20], [21], which showed that the strong and weak absorption bands of the (S - S) bond are located between (543-809) cm^{-1}, while the bands located (1100-1630) cm^{-1} are due to the (Mo-S) bond, while the bands located (2740-2357) cm^{-1} are due to the (O-H) bond.

4 CONCLUSIONS

Sol-gel was used to make molybdenum disulfide nanoparticles (MoS2) for this work. Transition metal dichalcogenides (MoS2) nanoparticles were prepared by sol-gel method using sodium molybdate dihydrate [Na2MoO4.2H2O] with thiourea (SC(NH2)2. The XRD examination yielded nanoparticles with an average size of 41 nm, which matched the particle size estimated from FESEM images, which was approximately 42 nm, therefore, MoS2 nanoparticles can be used in the field of batteries and catalysts. The average size distribution of MoS2 is about 42 nm. These results are consistent with the XRD. FTIR measurements performed for MoS2 nanoparticles showed that the strong and weak absorption bands of the (S - S) bond are located between (543-809) cm^{-1}, while the bands located (1100-1630) cm^{-1} are due to the (Mo-S) bond, while the bands located at (2740-2357) cm^{-1} are due to the (O-H) bond

REFERENCES

[1] X. Duan and H. Zhang, "Introduction: two-dimensional layered transition metal dichalcogenides," Chem. Rev., vol. 124, no. 19, pp. 10619-10622, 2024.

[2] S. Peng, C. Zhang, Y. Wei, Y. Ouyang, J. Han, C. Li, M. Dong, and J. Wang, "High-performance self-powered PbSe/WSe2 pn heterojunction photodetector for image sensing," J. Mater. Sci. Technol., vol. 225, pp. 125-132, 2025.

[3] S. Joseph, J. Mohan, S. Lakshmy, S. Thomas, B. Chakraborty, S. Thomas, and N. Kalarikkal, "A review of the synthesis, properties, and applications of 2D transition metal dichalcogenides and their heterostructures," Mater. Chem. Phys., vol. 297, p. 127332, 2023.

[4] D. Lucio-Rosales, D. Torres-Torres, and A. Garcia-Garcia, "A focused study of the out-plane mechanical properties and the spiral growth of MoS2 structures," Surf. Coat. Technol., p. 132034, 2025.

[5] Q. Tao, R. Wu, X. Zou, Y. Chen, W. Li, Z. Lu, L. Ma, L. Kong, D. Lu, X. Yang, and W. Song, "High-density vertical sidewall MoS2 transistors through T-shape vertical lamination," Nat. Commun., vol. 15, no. 1, p. 5774, 2024.

[6] F. Cui, V. García-López, Z. Wang, Z. Luo, D. He, X. Feng, R. Dong, and X. Wang, "Two-Dimensional Organic-Inorganic van der Waals Hybrids," Chem. Rev., vol. 125, no. 1, pp. 445-520, 2024.

[7] H. Mao, Y. Fu, H. Yang, S. Zhang, J. Liu, S. Wu, Q. Wu, T. Ma, and X. M. Song, "Structure-activity relationship toward electrocatalytic nitrogen reduction of MoS2 growing on polypyrrole/graphene oxide affected by pyridinium-type ionic liquids," Chem. Eng. J., vol. 425, p. 131769, 2021.

[8] S. M. Jassim, A. A. Mohammed, M. M. Kareem, and Z. T. Khodair, "Synthesis and characterization of Cr-doped cadmium oxide thin films for NH3 gas-sensing applications," Bull. Mater. Sci., vol. 47, no. 2, p. 104, 2024.

[9] A. M. Mohammad, H. S. Ahmed Al-Jaf, H. Sh. Ahmed, M. M. Mohammed, and Z. T. Khodair, "Structural and morphological studies of ZnO nanostructures," J. Ovonic Res., vol. 18, no. 3, pp. 443-452, May-June 2022.

[10] A. A. Mohammed, M. A. Ahmed, and S. M. Jassim, "Preparation and investigation of the structural and optical characteristics of manganese-doped cadmium oxide films," Digest J. Nanomater. Biostruct., vol. 18, no. 2, pp. 613-625, 2023.

[11] Z. Chen, T. Dedova, I. O. Acik, M. Danilson, and M. Krunks, "Nickel oxide films by chemical spray: Effect of deposition temperature and solvent type on structural, optical, and surface properties," Applied Surface Science, vol. 548, p. 149118, 2021, doi: 10.1016/j.apsusc.2021.149118.

[12] M. Araya Mungchamnankit, P. Eiamchai, C. Chananonnawathorn, S. Limwichean, M. Horprathum, A. Thongmee, and P. Sukplang, "Effect of annealing temperature on structural, morphological and optical properties of ZnO nanorod thin films prepared by hydrothermal method," Advanced Materials Research, vol. 979, pp. 204-207, Jun. 2014, doi: 10.4028/www.scientific.net/AMR.979.204.

[13] Y. Guo, X. Wang, H. Lei, Z. Tan, and J. Chen, "Characterization of evaporated tin sulfide and its application for hybrid solar cell," Materials Letters, vol. 251, pp. 234-237, 2019, doi: 10.1016/j.matlet.2019.05.036.

[14] Z. Feng, P. Yang, G. Wen, H. Li, Y. Liu, and X. Zhao, "One-step synthesis of MoS2 nanoparticles with different morphologies for electromagnetic wave absorption," Appl. Surf. Sci., vol. 502, p. 144129, 2020.

[15] F. M. Abdul Razzaq and A. S. Jabur, "Evaluation of α-Alumina nanoparticles prepared by sol-gel method," Basrah Journal for Engineering Sciences, vol. 24, no. 2, pp. 1-4, 2024.

[16] X. Guo, Z. Wang, W. Zhu, and H. Yang, "The novel and facile preparation of multilayer MoS2 crystals by

a chelation-assisted sol-gel method and their electrochemical performance," RSC Adv., vol. 7, no. 15, pp. 9009-9014, 2017.

[17] A. Yadav, A. K. Sharma, J. Yadav, S. Bhasker, G. Mishra, H. P. Bhasker, S. P. Patel, P. K. Dhawan, and D. K. Chaudhary, "Morphological impact on energy storage properties of 2D-MoS2 and its nanocomposites: a comprehensive review," Zeitschrift für Naturforschung A, 2025.

[18] R. Aggarwal, D. Saini, R. Mitra, S. K. Sonkar, A. K. Sonker, and G. Westman, "From bulk molybdenum disulfide (MoS2) to suspensions of exfoliated MoS2 in an aqueous medium and their applications," Langmuir, vol. 40, no. 19, pp. 9855-9872, 2024.

[19] M. Yi and C. Zhang, "The synthesis of two-dimensional MoS2 nanosheets with enhanced tribological properties as oil additives," RSC Adv., vol. 8, no. 17, pp. 9564-9573, 2018.

[20] K. C. Lalithambika, K. Shanmugapriya, and S. Sriram, "Photocatalytic activity of MoS2 nanoparticles: an experimental and DFT analysis," Appl. Phys. A, vol. 125, pp. 1-8, 2019.

[21] K. E. Ramohlola, E. I. Iwuoha, M. J. Hato, and K. D. Modibane, "Instrumental techniques for characterization of molybdenum disulphide nanostructures," J. Anal. Methods Chem., vol. 2020, p. 8896698, 2020.